PHYSICAL REVIEW A VOLUME 26, NUMBER 1 JULY 1982

Electronic spin relaxation of the $4^2S_{1/2}$ state of K induced by K-He and K-Ne collisions

F. A. Franz and C. Volk*
Department of Physics, Indiana University, Bloomington, Indiana 47405

(Received 30 November 1981)

Electronic and nuclear spin relaxation of optically pumped K atoms has been measured in the presence of He and Ne gases. The nuclear-spin-independent cross sections for the destruction of electronic spin polarization in the $4^2S_{1/2}$ ground state of K are $\sigma[\gamma(\vec{S}\cdot\vec{N})](\text{K-He}) = 8.0\times10^{-25}$ cm^2 and $\sigma[\gamma(\vec{S}\cdot\vec{N})](\text{K-Ne}) = 141\times10^{-25}$ cm^2. The diffusion coefficients of K in He and Ne, corrected to 273 K, are $D_0(\text{K-He}) = 0.35$ cm^2 sec^{-1} and $D_0(\text{K-Ne}) = 0.19$ cm^{2}sec^{-1}. All measurements have an estimated uncertainty of $\pm10\%$. The relaxation of K is shown to be strongly affected by an anomalous process which is attributed to the modification of the K hyperfine interaction induced by the formation of K-He and K-Ne van der Waals complexes.

I. INTRODUCTION

The best known cause of electronic spin relaxation in sudden binary collisions of alkali-metal atoms with noble-gas atoms is the effective spin-orbit interaction $\gamma(\vec{S}\cdot\vec{N})$, induced between $\vec{S}$, the spin of the valence electron of the alkali-metal atom, and $\vec{N}$, the angular momentum of the alkali-metal atom and the noble-gas atom around each other.[1-4] The $\gamma(\vec{S}\cdot\vec{N})$ interaction is important both in sudden binary collisions and in molecule-forming or "sticky" collisions.[5] In the case of Rb in moderate pressures of He and Ne, however, the dominant mode of relaxation has been shown to be an anomalous process, attributed to the modification of the Rb hyperfine interaction in the formation of Rb-He and Rb-Ne van der Waals molecules.[6-8] Recent measurements of the relaxation of ^{85}Rb and ^{87}Rb at high magnetic fields confirm the importance of this anomalous effect, and lend support to its molecular interpretation.[9]

We have used low magnetic field white light optical pumping to measure the electronic and nuclear-spin relaxation of the $4^2\,S_{1/2}$ state of K. Our primary interest lay in determining the degree to which anomalous relaxation might exist in an alkali metal with a significantly smaller hyperfine interaction than Rb. A secondary interest was that spin-relaxation rates for potassium had been measured previously only in He, and had been evaluated at a time when the influence of nuclear-spin mechanics on optical pumping transients was not fully appreciated. There was the promise, therefore, also of gaining new information on the $\gamma(\vec{S}\cdot\vec{N})$ cross sections for K.

We report here measurements of the spin relaxation of the $4^2\,S_{1/2}$ state of K in He and Ne buffer gases at pressures ranging from 1 to 600 Torr. We determine the relevant diffusion coefficients and cross sections for $\gamma(\vec{S}\cdot\vec{N})$ relaxation. We find that anomalous relaxation is present for K in He and Ne, although to a smaller degree than for Rb in these gases.

II. MEASUREMENTS OF $\langle S_z\rangle_g$ PUMPING TRANSIENTS

Our experiment involves $\sigma^+\ D_1$ white light optical pumping of K. We made measurements using the relatively standard transmission monitoring optical pumping apparatus described in Ref. 10; only the features relevant for K are described here. As usual, the optical pumping transient monitored the evolution of $\langle S_z\rangle_g$, the ground-state electronic spin polarization of the alkali-metal vapor.

A. Pumping cell

The optical pumping cell was a pyrex cylinder of inner dimensions 6.90 cm in diameter and 8.25 cm in length, situated in a magnetic field of 0.21 G. The all-metal and glass-gas handling system initially was baked at 360 °C for a minimum of 12 h: The ultimate vacuum obtained was 1.0×10^{-7} Torr. Following bakeout, dry nitrogen was admitted to the system and the chloride of the appropriate K isotope plus calcium shavings were placed in a sidearm. After resealing and several subsequent hours of pumping, the K was distilled under vacuum into the cell, and the sidearm was drawn off.

The cell was surrounded by a thermally insulated box, with optical access provided by two 3-in. diameter holes into which evacuated pyrex cylinders were sealed. The cell was heated by a noninductive element and was maintained to within ±0.1 °C by a temperature controller.

B. Detection of the transient pumping signal

The pumping beam was similar to that described in Ref. 10, with K D_1-pass (7699- Å) filters replacing the corresponding Cs filters. Changes in the transmitted light intensity were monitored by observing the voltage drop across a 500-kΩ resistor of the current from an unbiased PIN 10D photodiode. The monitoring signal was fed into one input of a PAR 113 ultralow-noise dc preamplifier. A balancing voltage from a mercury-cell potentiometer was fed into the other input. Optical pumping transients ranged from a few parts in 10^6 to a few parts in 10^4 of the intensity of light incident upon the photodetector.

The differentially amplified signal was fed into the dc input of a signal averager. The timing of the experiment was controlled by the signal averager. At the end of each sweep the averager produced a synchronous pulse which triggered a single cycle of a low-frequency square wave from a function generator. The square wave gated another function generator which throughout the initial half cycle supplied sinusoidal rf power (137 kHz for the K isotopes) to a modified Helmholtz coil mounted on the optical pumping cell, saturating the ground-state Zeeman resonance in both the $F=2$ and $F=1$ hyperfine sublevels. The sweep of the signal averager thus provided an initial baseline (rf power on) followed by the optical pumping transient (rf off). Depending on the signal size, between 2^{11} and 2^{15} sweeps were averaged.

We used the low-frequency roll off (0.03 Hz) on the PAR preamplifier to block small drifts in the dc light level. Since no single sweep time was longer than 2.0 sec, no discernable distortion of the signal was introduced by this procedure. The ambient room temperature was controlled during the experimental run in order to ensure constancy of filter transmission and degree of light polarization. Before each run the circular polarization of the pumping beam was checked by placing a linear polarizer in the beam. Adjustments of circular polarization were made until rotation of the linear polarizer produced an intensity change of 1% or less.

C. Extraction and analysis of the experimental data

The signal averager stored and averaged the pumping signal in 1000 digitized channels. Data acquired from each run was punched onto paper tape, read into the computer, and fit by Eq. (2). In addition to normal statistical analyses, a plot of the theoretical fit was plotted on top of the experimental data for each run to provide a visual check of the "goodness" of the fit.

III. RESULTS AND DISCUSSION

A. Pumping equations

The most important interactions contributing to relaxation of optically pumped alkali-metal vapors are various kinds of collisions of pumped atoms with the walls of the cell, with buffer gas atoms, and with unpumped atoms (spin exchange). Collisions may be binary and sudden in nature, or may be "sticky" or multiple body resulting in the formation of quasimolecular complexes. Interactions both in the ground state and in the excited state influence the course of optical pumping.

It has been shown in earlier work that if the optical pumping rate is small compared to typical relaxation rates (weak pumping limit), then the rate of change of the electronic and nuclear-spin polarizations of the vapor, $\langle S_z \rangle_g$ and $\langle I_z \rangle_g$, are governed by the following equations[7]:

$$\frac{d\langle S_z \rangle_g}{dt} = B_1 - B_2\langle S_z \rangle_g + B_3\langle I_z \rangle_g \ , \tag{1a}$$

$$\frac{d\langle I_z \rangle_g}{dt} = C_1 - C_2\langle I_z \rangle_g + C_3\langle S_z \rangle_g \ , \tag{1b}$$

where the B_i and C_i are functions of the various relaxation rates and of the pumping rate. The coupling between Eqs. (1a) and (1b) is caused by nuclear-spin mechanics pertinent to certain types of collisions.

The solution to Eqs. (1a) and (1b) for $\langle S_z \rangle_g$, the optical pumping transient observed in this experiment, is

$$\langle S_z \rangle_g = D_1[1-\exp(-Z_1 t)] + D_2(1-\exp(-Z_2 t)] \ , \tag{2}$$

assuming that $\langle S_z \rangle_g \ (t=0) = \langle I_z \rangle_g (t=0) = 0$. The solutions for the rate constants Z_1 and Z_2 are

$$Z_1 = \tfrac{1}{2}\{ (B_2+C_2) - (B_2-C_2)[1+4B_3C_3(B_2-C_2)^{-2}]^{1/2} \} \ , \tag{3a}$$

$$Z_2 = \tfrac{1}{2}\{ [B_2+C_2) + (B_2-C_2)[1+4B_3C_3(B_2-C_2)^{-2}]^{1/2} \} \ . \tag{3b}$$

The solutions for the parameters D_1 and D_2 are given in Ref. 7.

Summaries of the contributions of all relevant relaxation mechanisms to the optical pumping transient have been published in Refs. 7 and 8. We use these results extensively in the present experiment. For both of the isotopes studied in the present experiment, ^{39}K and ^{41}K, the results for $I=\frac{3}{2}$ apply. We list below the relaxation mechanisms relevant to the present experiment and indicate their approximate contributions to Z_1 and Z_2 the "slow" and "fast" rate constants, respectively.

1. $\gamma(\vec{S}\cdot\vec{N})$ relaxation in sudden binary collisions of ground-state K atoms with He or Ne atoms makes a full contribution R, to Z_2, but only R/8 to Z_1. The explicit form of R is

$$R = N_0 \sigma v_{\text{rel}} \frac{p}{p_0} \ , \tag{4}$$

where N_0 is Loschmidt's number at the temperature of the experimental cell, σ is the nuclear-spin independent cross section for the destruction of $\langle S_z \rangle_g$, v_{rel} is the mean relative velocity of K atoms and buffer gas atoms, p is the pressure of the buffer gas, and p_0 is atmospheric pressure.

The nuclear-spin mechanics of R are of the form

$$\frac{d\langle S_z \rangle_g}{dt} = -R\langle S_z \rangle_g + (R/8)\langle I_z \rangle_g \ , \tag{5a}$$

$$\frac{d\langle I_z \rangle_g}{dt} = -(R/8)\langle I_z \rangle_g \ . \tag{5b}$$

2. Anomalous relaxation R^*, in the K ground state makes a full contribution to Z_2, but no contribution to Z_1. The postulated and apparent nuclear-spin mechanics of R^* are

$$\frac{d\langle S_z \rangle_g}{dt} = -R^*\langle S_z \rangle_g + (R^*/5)\langle I_z \rangle_g \ , \tag{6a}$$

$$\frac{d\langle I_z \rangle_g}{dt} = -(R^*/5)\langle I_z \rangle_g + R^*\langle S_z \rangle_g \ . \tag{6b}$$

3. Relaxation resulting from diffusion of K to the walls of the cell R', makes equal contributions to Z_2 and Z_1. The explicit form of R' is

$$R' = [(\pi/L^2 + (2.405/r)^2] D_0 P_0 / p \ , \tag{7}$$

where L and r are the length and radius of the cell, and D_0 is the diffusion coefficient of K in the buffer gas at atmospheric pressure and at the temperature of the cell. The nuclear-spin mechanics of R' are

$$\frac{d\langle S_z \rangle_g}{dt} = -R'\langle S_z \rangle_g \ , \tag{8a}$$

$$\frac{d\langle I_z \rangle_g}{dt} = -R'\langle I_z \rangle_g \ . \tag{8b}$$

4. K-K spin exchange R_s, makes a strong contribution to Z_2, but essentially no contribution to Z_1. The explicit form of R_s is

$$R_s = n_0 \sigma_s v_{K-K} \frac{p_K}{p_0} \ , \tag{9}$$

where σ_s is the nuclear-spin independent cross section for spin exchange in K-K collisions, v_{K-K} is the mean relative velocity of colliding K atoms, and p_K is the vapor pressure of K. The nuclear-spin mechanics of R_s are

$$\frac{d\langle S_z \rangle_g}{dt} = -(5/8)R_s\langle S_g \rangle_g + (R_s/8)\langle I_z \rangle_g \ , \tag{10a}$$

$$\frac{d\langle I_z \rangle_g}{dt} = -(R_s/8)\langle I_z \rangle_g + (5/8)R_s\langle S_z \rangle_g \ . \tag{10b}$$

5. Collisional relaxation of K atoms within the $^2P_{1/2}$ excited state affects only B_1 and C_1 and hence plays a role only in determining the ratio of amplitudes D_1/D_2, in the $\langle S_z \rangle_g$ transient. The important parameters are the rate of collisional relaxation within the $^2P_{1/2}$ state Γ_1, and the mean lifetime of the $^2P_{1/2}$ state τ. We have

$$\Gamma_1 = n_0 \Lambda_2 v_{vel} \frac{p}{p_0} \ , \tag{11}$$

where Λ_1 is the nuclear-spin independent cross section for the destruction of orientation in the $^2P_{1/2}$ state.

6. The pumping rate $A/3$, makes equal contribu-

tions to Z_1 *and* Z_2. For the sake of completeness and convenience, we summarize the contributions of these various relaxation mechanisms to the B_i and C_i of Eqs. (1a) and (1b) (Refs. 7, 8, and 10):

$$B_1=A[\tfrac{1}{16}+\tfrac{1}{36}(3\Gamma_1\tau-1)(1+\Gamma_1\tau)^{-1}(8+\Gamma_1\tau)^{-1}] , \tag{12a}$$

$$B_2=A/3+R+R'+5R_s/8+R^* , \tag{12b}$$

$$B_3-R/8+R_s/8+R^*/5 , \tag{12c}$$

$$C_1=A[\tfrac{5}{48}+\tfrac{25}{36}(8+\Gamma_1\tau)^{-1}] , \tag{13a}$$

$$C_2=A/3+R/8+R'+R_s/8+R^*/5 , \tag{13b}$$

$$C_3=5R_s/8+R^* . \tag{13c}$$

B. Determination of relaxation parameters for K in He

In Fig. 1 we display measurements of the slow and fast relaxation rates Z_1 and Z_2, for optically pumped ^{39}K in He over the range of He pressures from 30 to 550 Torr. R, the binary $\gamma(\vec{S}\cdot\vec{N})$ relaxation rate, already small for K-He, makes almost negligible contributions to Z_1 over the range of pressures studied, being reduced by the nuclear-spin "slowing factor" 1/8. Z_1 therefore reflects mainly the wall relaxation rate R', and the pumping rate $A/3$. Z_2 reflects R' and $A/3$, and, in addition, contains full contributions from R and R_2. A "hump" in the Z_2 data between 100 and 300 Torr is prominent: This maximum is similar to that observed for R^* of Rb in He,[6] and has the properties of anomalous relaxation, that is, a strong contribution to Z_2, but no discernable contribution to Z_1.[8]

Wall relaxation is the dominant mode of relaxation at low buffer pressures, and Z_1 and Z_2 approach a common value. It has been shown that in this case the double exponential $\langle S_z\rangle_g$ transient can be approximated very well by a single exponential with rate constant Z_3, where[10]

$$Z_3\cong(D_1Z_1+D_2Z_2)(D_1+D_2)^{-1} . \tag{14}$$

In Fig. 2 we display measurements of effective single exponential relaxation rates of ^{39}K and ^{41}K in low pressures of He. The solid curve in Fig. 2 is a fit of Eq. (14) to the data, with the following values taken for various relaxation parameters:

$\sigma_s=1.45\times10^{-14}$ cm^2, (Ref. 11)

$p(K)=2.9\times10^{-7}$Torr at 325 K, (Ref. 12)

$\Lambda_1(4^2P_{1/2},\mathrm{K-He})=24\times10^{-16}$ cm^2, (Ref. 13)

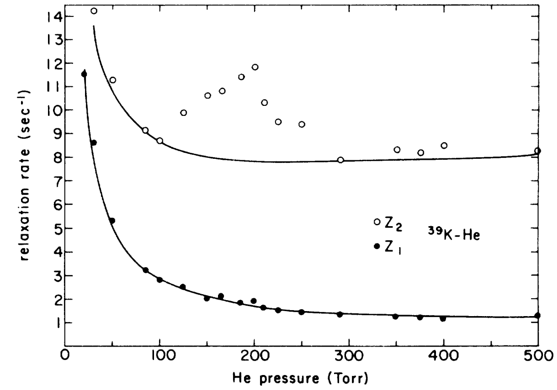

FIG. 1. Measured relaxation rates Z_1 and Z_2, for ^{39}K in He. Each data point represents the average of three to five separate measurements. The standard deviations are less than 5% for the Z_1 data, and less than 10% for the Z_2 data. The solid curves are calculations of Z_1 and Z_2 ignoring anomalous relaxation, as discussed in the text.

$\tau(4^2P_{1/2},\mathrm{K})=2.77\times10^{-8}$ sec , (Ref. 14)

$A/3=0.45$ sec^{-1} .

The only parameter unspecified was the wall relaxation rate R'. The fit yielded $R'=(232/p)$ Torr sec^{-1}, implying that

$$D_0(\mathrm{K-He},325\,°\mathrm{K})=0.45\ \mathrm{cm^2\,sec^{-1}} .$$

Assuming a $T^{3/2}$ dependence of D_0, we obtain

$$D_0(\mathrm{K-He},273°\mathrm{K})=0.35\ \mathrm{cm^2\,sec^{-1}} .$$

Extraction of a $\gamma(\vec{S}\cdot\vec{N})$ cross section from the Z_2 data is complicated by the considerably greater strength of anomalous relaxation compared to normal $\gamma(\vec{S}\cdot\vec{N})$ relaxation at moderate pressures of He. Z_1 data, in which R^* contributions are absent, appear to be a better choice for such an analysis. Within the range of He pressures available to us, however, $R/8$ is small compared to other relaxation rates, making a determination of $\sigma[\gamma(\vec{S}\cdot\vec{N})]$ uncertain also in this case. For K-He therefore, we utilize high-pressure data from another experiment to determine $\sigma[\gamma(\vec{S}\cdot\vec{N})]$ and demonstrate compatibility of that value with the present measurements.

In 1965, Bernheim and Korte (BK) measured rates of relaxation of K in He at pressures ranging up to 1900 Torr, and reported a cross section σ (K-He) of 1.1 $\times$ 10^{-25} cm^2.[15] The higher pressures at which BK worked make their data more sensitive to σ than are ours, and hence their data should lead to a more reliable determination of this cross section. BK did not consider nuclear-spin effects in their

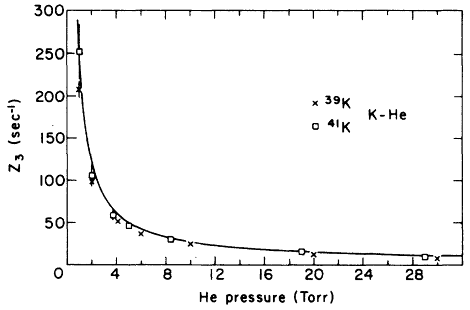

FIG. 2. Measured effective single exponential relaxation rates Z_3, for ^{39}K and ^{41}K in low pressures of He. The solid curve is a fit of Eq. (14) to the data, as discussed in the text.

analysis, however, so the evaluation of their data must be reconsidered. It is important, first, to make clear exactly what observable BK measured.

Using Eqs. (3a), (3b), and (12a) through (13c) above and Eq. (21) of Ref. 7, it is not difficult to show that when R_s becomes large, Z_2 becomes large, Z_1 remains essentially unaffected, and the D_1/D_2 ratio approaches infinity. The relaxation transient then becomes effectively a single exponential, with a rate constant equal to Z_1. BK's experiment was performed at 85 °C, at which temperature we estimate the K-K spin exchange rate R_s, to be approximately 140 sec^{-1}.[11,12] We calculate that the D_1/D_2 ratio must have been about 64. Z_1 therefore is the parameter that BK actually measured. R for K-He does not make a full contribution to Z_1, however; it is reduced by the nuclear-spin factor. The cross section reported by BK, therefore, corresponds not to $\sigma[\gamma(\vec{S}\cdot\vec{N})]$, but rather to $\sigma[\gamma(\vec{S}\cdot\vec{N})]/8$. A more careful evaluation indicates that a value of $\sigma[\gamma(\vec{S}\cdot\vec{N})]=8.0\times10^{-25}$ cm^2 best fits BK's high-pressure data. This value is consistent also with our own data, as we show in Fig. 1. The solid curves through the Z_1 and Z_2 data in Fig. 1 are calculated from Eqs. (3a) and (3b), based on the relaxation parameters listed above and taking $\sigma[\gamma(\vec{S}\cdot\vec{N})]$ to be 8.0×10^{-25} cm^2.

The present data provide the best determination of the diffusion coefficient, however. The value of D_0(K-He) found by Bernheim and Korte was 1.2 cm^2/sec, or 0.80 cm^2/sec extrapolated to 273° K, much higher than the value that we report. The difference almost certainly is due to the higher temperature and thus higher vapor pressure at which BK worked, 85 °C compared to 52 °C in the present experiment. The vapor pressure of K changes by a factor of almost 20 over this temperature range. At higher vapor pressures, optical pumping occurs primarily near the front of the cell rather than uniformly throughout it. Analyses have shown that spuriously high determinations of D_0 result from measurements of relaxation transients under such conditions.[16]

C. Determination relaxation parameters for K in Ne

In Fig. 3 we display measurements of Z_1 and Z_2 for ^{41}K in Ne. As was the case for K in He, there is a pronounced anomalous effect in the Z_2 data, making this data unsuitable for an accurate determination of $\sigma[\gamma(\vec{S}\cdot\vec{N})]$. This cross section for K-Ne, however, is considerably larger than the corresponding cross section for K-He; its influence on Z_1 is substantial at high Ne pressures. As a consequence we can fit Eq. (3a) to the Z_1 data, ultimately determining both $\sigma[\gamma(\vec{S}\cdot\vec{N})]$ (K-Ne) and D_0(K-Ne). These values are summarized in Table I. The solid curves in Fig. 3 represent the result of the fit to the Z_1 data, and the result of calculation of Z_2 with all relaxation parameters now fixed. Anomalous relaxation has been neglected in these calculations.

The low-pressure effective single exponential transients [Eq. (14)] were used as a check of the determination of the diffusion coefficient. The data and the calculations are displayed in Fig. 4. For these calculations we used $\Lambda_1(\text{K-He})(^2P_{1/2})=21\times10^{-16}$ cm^2.[13] The average pumping rate $A/3$ for the Ne measurements was 0.50 sec^{-1}.

D. Anomalous relaxation

Having determined values of D_0 and $\sigma[\gamma(\vec{S}\cdot\vec{N})]$ for K in He and K in Ne, it is possible to extract

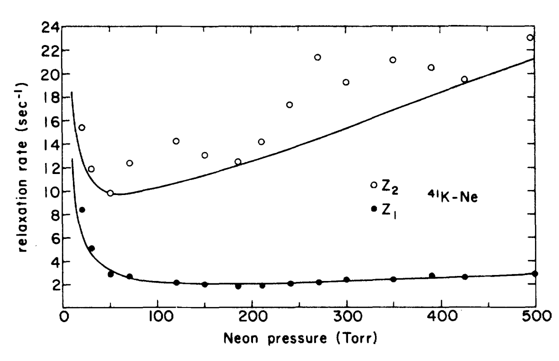

FIG. 3. Measured relaxation rates Z_1 and Z_2, for ^{41}K in Ne. Each data point represents the average of three to five separate measurements. The standard deviations are less than 5% for the Z_1 data, and less than 10% for the Z_2 data. The solid curves are calculations of Z_1 and Z_2 ignoring anomalous relaxation, as discussed in the text.

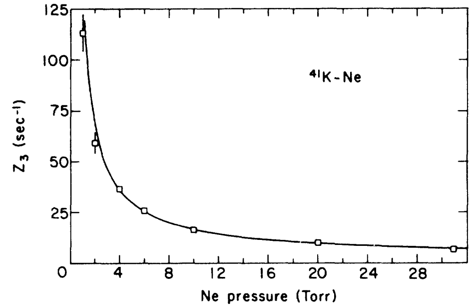

FIG. 4. Measured effective single exponential relaxation rates Z_3 for ^{41}K in Ne. Low pressures of Ne. The solid curve is a fit of Eq. (14) to the data, as discussed in the text.

values of the rate of anomalous relaxation R^*, by determining those values of R^* required to bring the calculated values of Z_2 [Eq. (3b)] into coincidence with the measured values. The nuclear-spin mechanics of R^* are of critical importance, of course, since they must be such as to provide a contribution to Z_2, but no contribution to Z_1. As in Ref. 8, we have taken the interaction to be of the type $\delta a(\vec{S}\cdot\vec{I})$, with nuclear-spin mechanics of the form given in Eqs. (6a) and (6b). The results of these calculations are presented in Figs. 5 and 6.

The influence of anomalous relaxation is mirrored also in the observable D_1/D_2, as we show in Figs. 7 and 8. The triangles in these figures represent calculations of D_1/D_2, using Eq. (21) of Ref. 7. We have taken the low magnetic field cross sections for relaxation within the $^2P_{1/2}$ state of K to be as measured by Niewitecka and Krause (see above), and the ground-state relaxation parameters as measured in this paper. There are *no* variable parameters in these calculations.[17]

TABLE I. Nuclear-spin independent relaxation cross sections and diffusion coefficients for optically pumped K in He and Ne.

	$\sigma[\gamma(\vec{S}\cdot\vec{N})]$ (10^{-25} cm^2)	D_0 (cm^2 sec^{-1} at 273 ° K)
K-He	8.0	0.35
K-Ne	141	0.19

Figures 5 and 6 make clear that anomalous relaxation plays important roles in K-He and K-Ne. For K-He, R^* at 200 Torr is about 3 sec^{-1} whereas $R[\gamma(\vec{S}\cdot\vec{N})]$ is about 0.66 sec^{-1}: At that pressure of He R^* is about 4.5 times greater than R. Similarly, at 100 Torr of Ne, R^* is about 3 sec $^{-1}$, whereas $R[\gamma(\vec{S}\cdot\vec{N})]$ is about 4 sec $^{-1}$; the contributions from the two relaxation processes are comparable. R^* is considerably less from the two relaxation processes are comparable. R^* is considerably less significant in K than in Rb, however, where the dominance of R^* over $R[\gamma(\vec{S}\cdot\vec{N})]$ can be by as much as a factor of 40.[6,7]

The R^* data for K-He and for K-Ne display marked maxima, but are too uncertain to yield accurate equilibrium values of R^* at high pressure. Figure 5 suggests that R^*(K-He) at high He pressure is about 0.5 sec^{-1}, but a value of zero cannot be excluded. Similarly, there appears that there could be a second maximum of R^*(K-Ne) in Fig. 6, but this apparent peak could equally well, within experimental uncertainty, be a rise of R^* to a constant value.

The data in Figs. 5 and 6 nevertheless are consistent with the attribution of R^* to van der Waals molecular formation. As explained in Refs. 6, 7, and 8, the most likely cause of maxima in R^* are contributions arising from the formation of quasi-

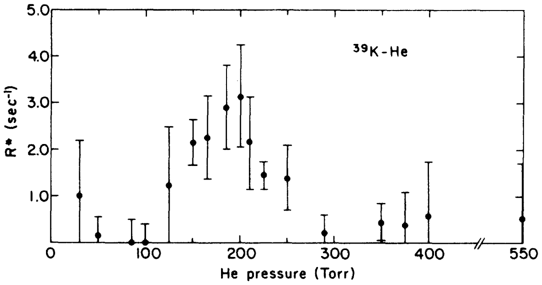

FIG. 5. Anomalous relaxation R^* for ^{39}K in He, evaluated from Z_2 data, as described in the text.

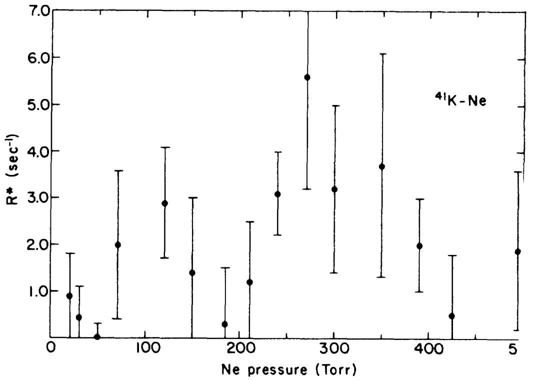

FIG. 6. Anomalous relaxation R^*, for ^{41}K in Ne, evaluated from Z_2 data, as described in the text.

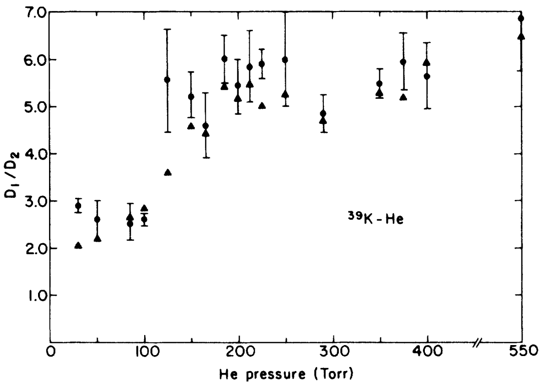

FIG. 7. Measured ratios of the two exponential contributions to the $\langle S_z \rangle_g$ transient D_1/D_2, for optically pumped ^{39}K in He. The triangles represent calculated values, as discussed in the text.

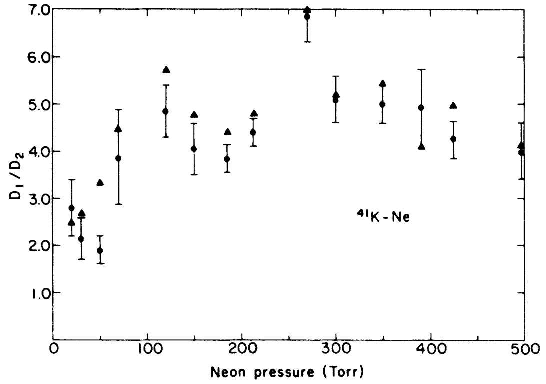

FIG. 8. Measured ratios of the two exponential contributions to the $\langle S_z \rangle_g$ transient D_1/D_2, for optically pumped ^{41}K in Ne. The triangles represent calculated values, as discussed in the text.

bound van der Waals molecules in two-body collisions. At low pressure the R^* relaxation rate is effectively proportional to the formation rate of complexes, thus proportional to p in the two-body case and to p^2 in the three-body case. At higher pressures the destruction rate determines the value of the correlation time τ_c. Reference to Eq. (3) of Ref. 8 shows that as $p \rightarrow \infty$, R^* should approach zero as $(1/p)$ in the two-body case, but should approach a constant value in the three-body case. The maximum in the K-He data in Fig. 5, therefore, suggests a strong contribution from quasibound molecules formed in two-body collisions. This possibility is supported by calculations based on the Baylis potential parameters which indicate that for K-He there should be a single quasibound state with sixfold degeneracy, and one bound state with two-fold degeneracy.[18]

A pressure dependence of R^* similar to that observed for K-Ne, a peak and a subsequent rise to a constant value, or two peaks, could be explained if the break-up cross sections for K-Ne molecules were substantially different for the various vibrational states of the molecule. Different cross sections would yield different values for τ_c, resulting in contributions to R^* which would differ in dependence upon pressure. Differences in cross sections could come about in the following way. For molecules in bound states, the break-up process must add energy in order to free the alkali-metal atom and noble-gas atom. The energies of quasibound states, however, are greater than zero. In that case a modest relatively long-range distortion of the interatomic potential may free the atoms, or may increase the probability for dissociation via tunneling. Breakup then should be represented by cross sections substantially larger than the cross section for breakup of bound-state molecules. More work obviously is necessary, however, if these speculations are to be confirmed.

ACKNOWLEDGMENT

This research was supported in part by the Air Force Office of Scientific Research under Grant No. 79-0031.

---

*Present address: Aerospace Corporation, P. O. Box 92957, Los Angeles, California 90009.

[1] R. A. Bernheim, J. Chem. Phys. 36, 135 (1962).

[2] R. M. Herman, Phys. Rev. 136, A1576 (1964).

[3] C. C. Bouchiat, M. A. Bouchiat, and L. C. L. Pottier, Phys. Rev. 181, 146 (1969).

[4] M. A. Bouchiat and J. Brossel, Phys. Rev. 147, 41 (1966).

[5] See, for example, C. C. Bouchiat and M. A. Bouchiat, Phys. Rev. A 2, 1274 (1970); and M. A. Bouchiat, J. Brossel, and L. C. Pottier, J. Chem. Phys. 56, 3703 (1972).

[6] F. A. Franz and C. Volk, Phys. Rev. Lett. 35, 1704 (1975).

[7] F. A. Franz and C. Volk, Phys. Rev. A 14, 1711 (1976).

[8] F. A. Franz and C. Volk, Phys. Rev. A 18, 599 (1978).

[9] F. A. Franz and A. Sieradzan, Phys. Rev. A 23, 2841 (1981).

[10] F. A. Franz and C. E. Sooriamoorthi, Phys. Rev. A. 10, 126 (1974).

[11] N. W. Ressler, R. H. Sands, and T. E. Stark, Phys. Rev. 184, 102 (1969).

[12] *Metals Reference Handbook,* edited by Colin J. Smithells (Butterworths, London, 1955), Vol. II, p. 613.

[13] B. Niewitecka and L. Krause, Can. J. Phys. 53, 1499 (1975).

[14] G. Copley and L. Krause, Can. J. Phys. 47, 533 (1969).

[15] R. A. Bernheim and M. W. Korte, J. Chem. Phys. 42, 2721 (1965).

[16] P. Minguzzi, F. Strumia, and P. Violino, Nuovo Cimento 46, 145 (1966).

[17] The calculations are not truly accurate representations of excited-state interactions; the collision rate at pressures above 20 Torr or so is greater than the hyperfine frequency of the excited state, and the nuclear-spin mechanics change character from those assumed to underlie the equations of Ref. 10. The effect on D_1/D_2, however, is small in comparison to the effect of R^* ground-state relaxation.

[18] W. E. Baylis, J. Chem. Phys. 51, 2665 (1969); corrected values by private communication.